Respiratory modulation of heart rate explains the magnitude but not the phase of respiratory modulation in arterial blood pressure

[1]William H. Barnett*, [1]Elizaveta Latash, [1]Robert Capps, [2]Erica A. Wehrwein, [3]Thomas E. Dick, [1]Yaroslav I. Molkov

[1]Georgia State University, Atlanta, GA, USA; [2]Michigan State University, East Lansing, MI, USA; [3]Case Western Reserve University, Cleveland, OH, USA

Introduction: Slow deep breathing (SDB) exercises may be a therapeutic intervention for wellness and wellbeing and can have measurable effects on cardiovascular activity. The mechanisms of action and putative therapeutic benefits of SDB are controversial. During SDB, the blood pressure decreases and the modulation of the blood pressure on the timescale of respiration increases [1]. These changes could be mediated by sympathetic input to the vasculature via sympathetic motor output controlling vasoconstriction or by respiratory modulated vagal input to the heart. Here, we focus on the second mechanism and test the hypothesis that respiratory modulation of the heart rate is sufficient to induce respiratory modulation in the arterial blood pressure.

Human respiratory and cardiovascular data

This dataset includes tidal volume, ECG, and arterial blood pressure from ten human participants [1]. Data was acquired for a spontaneous normal breathing experimental epoch, a slow deep breathing experimental epoch, and then a recovery epoch of normal breathing.

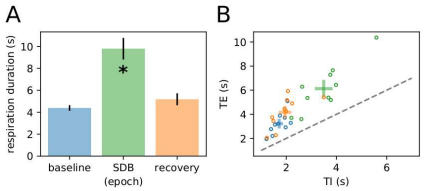

Figure 1. We verified that participants indeed substantially increased their period breathing (A), and we quantified the phase duration of breathing in the three experimental epochs (B). The baseline normal breathing epoch, the slow deep breathing epoch, and the recovery normal breathing epochs are blue, green, and orange respectively. In panel B, the dotted line is a line of slope one that passes through the origin. On average, the expiratory duration (TE) was greater than the inspiratory duration (TI) for all three experimental epochs for each participant. In so doing, we captured the time of the phase transitions from inspiration to expiration and from expiration to inspiration.

Methods: analysis of cardiovascular metrics

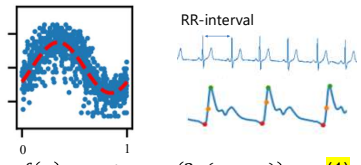

$$f(\varphi) = a_0 + a_1 \cos(2\pi(\varphi - a_2)) \qquad (1)$$

Figure 2. We quantified the respiratory modulation of cardiovascular metrics with a cosine tuning curve. The coefficient a_0 quantified the mean value of the metric. The coefficient a_1 quantified the depth of respiratory modulation of the metric. The coefficient a_2 quantified the phase offset of the metric from the inspiratory-to-expiratory phase transition. For each respiratory cycle, we computed the respiratory phase of cardiovascular events. Then we fit this cosine tuning curve to the data (blue data points and dashed red curve). The metrics analyzed in this manner were RR-interval (RRI; the difference between successive R-peaks in the ECG), the mean arterial pressure (MAP), and the pulse pressure (PP; the difference between end systole and end diastole pressures—green and red markers in sample blood pressure trace).

Methods: computational models of arterial pressure

We modeled the arterial pressure of individual human participants by feeding heartbeat times (Model #1) or heartbeat times and our analysis of a cardiovascular metric (Model #2) to our computational models. In both models, heart beat times was produced by adding 300 ms to the time of R-peaks in order to account for the short lag between each R-peak and the subsequent end-systole pressure event.

Model #1

$$\dot{p} = [p_0 - p]/\tau_p + PP \sum_i \delta(t - t_i) \qquad (2)$$

Equation (2) models arterial blood pressure (p) as a function of heart beat timings. The parameters p_0 and τ_p determined blood pressure dynamics between heart beats. At the time of the heart beat (t_i), the arterial pressure was incremented by the pulse pressure PP, which was fixed. $\dot{p}$ is the time derivative of arterial pressure (p).

Model #2

$$\dot{p} = [p_0 - p]/\tau_p + \sum_i f_{PP}(\varphi_i)\, \delta(t - t_i) \qquad (3)$$

Equation (3) models arterial blood pressure (p) as a function of heart beat timings. It differed from Model#1 in that the pulse pressure (f_{PP}) is here a function of the respiratory phase of the heartbeat (φ_i):

$$f_{PP}(\varphi) = PP_0 + PP_1 \cos(2\pi(\varphi - PP_2))$$

The coefficients PP_0, PP_1, and PP_2 were drawn from the cosine tuning curve fit of each individual human's arterial pressure data, and φ was the phase of that heart beat in the contemporaneous respiratory cycle triggered by the inspiration-to-expiration phase transition.

Respiratory modulation of cardiovascular metrics in human data

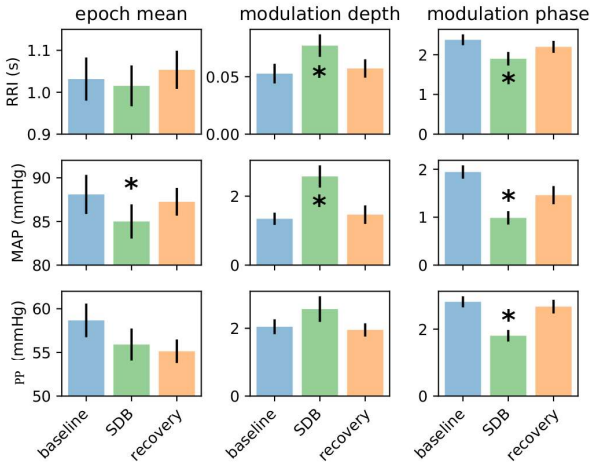

Figure 3. We characterized the respiratory modulation of RR-interval (RRI), mean arterial pressure (MAP), and arterial pulse pressure (PP) in each experimental epoch for all human participants. The data represented in this figure maps directly to the coefficients in equation (1) described in the methods. The first column depicts the group means for each metric in each of the three experimental epochs. This quantity is coefficient a_0 from equation (1). The second column depicts the group mean of the depth of respiratory modulation for each metric. This quantity is the coefficient a_1 from equation (1). The third column depicts the group mean of the phase offset of each metric from the inspiration-to-expiration phase change (depicted here in units of radians). This is the coefficient a_2 from equation (1).

Summary of results:

The depth and phase offset of respiratory modulation of RRI changed significantly during slow deep breathing. The mean, the modulation depth, and the modulation phase offset of MAP all changed significantly during slow deep breathing. The respiratory modulation phase offset of PP significantly changed during slow deep breathing.

Exemplar activity of arterial pressure computational models

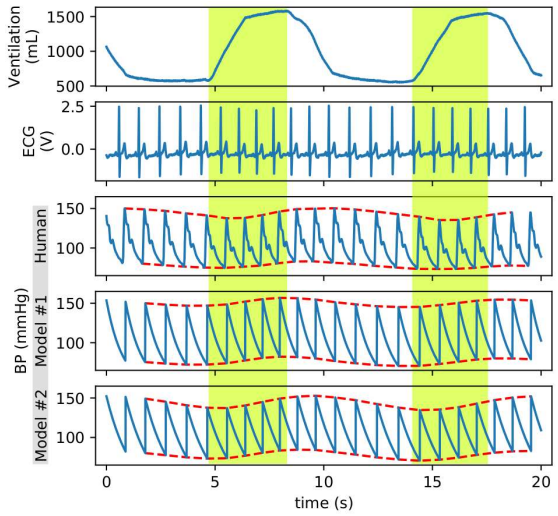

Figure 4. Depiction of human tidal volume, ECG, and arterial blood pressure during a slow deep breathing experimental epoch. This ECG and arterial pressure data was used to produce simulations of Model #1 and Model #2. In Model #1, only the heart beat times were used to produce a synthetic arterial pressure. In Model #2, both the heart beat times and the results of our analysis of respiratory modulation in arterial PP were used to produce a synthetic arterial pressure (see Methods equation (3)). The envelope of end-systole pressure and end-diastole pressure is depicted by dashed red lines in the human arterial pressure and the output of each of the two models. The inspiratory phase of respiration is highlighted by yellow stripes. Notice in the human BP trace that the distance between two dashed red curves (representing the end-systole pressures and the end-diastole pressures) is changing in time with the respiratory cycle. This is respiratory modulation of arterial PP, which does not appear in the output of Model #1 but is explicitly included in Model #2.

Exemplar respiratory modulation of model output compared to human data

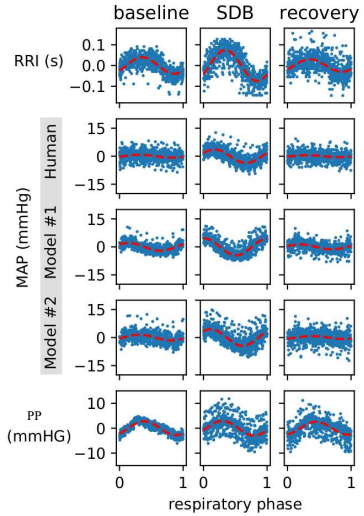

Figure 5. Example of respiratory modulation in human participants and model cardiovascular metrics. In each panel, the mean of the metric data (blue points) is subtracted to easily visualize the depth and phase offset of the respiratory modulation of each metric (RRI, MAP, PP). The red curve represents the cosine tuning curve fit to the data in that panel (see Figure 2 and equation (1)). The MAP of Model#1 qualitatively captures the depth of the respiratory modulation apparent in the human MAP, but it is clearly modulated at a different respiratory phase. The modulation of MAP in Model #2—which includes respiratory modulation of PP—captures both the depth and the phase offset of respiratory modulation.

Performance of computational models

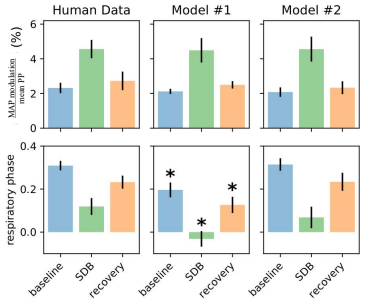

Figure 6. We quantified the performance of the computational models using two performance metrics: (1) the depth of MAP modulation in units of arterial PP and (2) the respiratory phase of MAP. In the first case, the models performed equally well, and we were not able to distinguish between either models and the human data in any of the three experimental epochs. In the second case, there was a clear deficit in the phase offset of respiratory modulation in Model #1 in comparison to the human data for all three of the experimental epochs. The discrepancy between Model #1 and the human data is clearly visible in the MAP phase diagrams in **Figure 5** as well as in the end-systole and end-diastole envelopes depicted in **Figure 4**.

Conclusions

We used a simple computational model of arterial blood pressure to show how respiratory modulation of the heart rate was sufficient to induce respiratory modulation in MAP using real human heartbeat times. To correct the phase difference, respiratory modulation of PP was required. These results support the hypothesis that respiratory modulation of MAP emerges from respiratory modulation of vagal tone to the heart, but phase modulation may require baroreceptor input or mechanical coupling between the heart and the lungs. We demonstrated how this mechanism supports increased cardio-respiratory coupling during SDB.

Acknowledgements

We gratefully acknowledge the support of NIH and the IMAG consortium supporting MSM U01EB021960-01 and NIH/NCCIH R01AT008632

References

Dick et al. *Respir Physiol Neurobiol.* 204, 2014.